

## Cross-linked Multilayer Polymer-Clay Nanocomposites and Permeability Properties

Bon-Cheol Ku,<sup>1</sup> Danielle Froio,<sup>2</sup> Diane Steeves,<sup>2</sup> Dong Wook Kim,<sup>3</sup>  
Heejoon Ahn,<sup>1</sup> Jo Ann Ratto,<sup>2</sup> Alexandre Blumstein,<sup>1</sup> Jayant Kumar,<sup>1,\*</sup>  
and Lynne A. Samuelson<sup>2,\*</sup>

<sup>1</sup>Center for Advanced Materials, Polymer Science Program, Departments of Chemistry  
and Physics, University of Massachusetts, Lowell, Massachusetts, USA

<sup>2</sup>US Army RDECOM, Natick Soldier Center, Natick, Massachusetts, USA

<sup>3</sup>Korea Research Institute of Chemical Technology, Daejeon, Korea

### ABSTRACT

Electrostatically layered aluminosilicate nanocomposites have been prepared by the sequential deposition of poly(allylamine hydrochloride)/poly(acrylic acid)/poly(allylamine hydrochloride)/saponite (PAH/PAA/PAH/saponite)<sub>10</sub> on poly(ethylene terephthalate) (PET) film. Exfoliated saponite nanoplatelets were obtained by extensive shaking, sonication, and centrifugation of a water suspension. To minimize permeability and improve the mechanical integrity, cross-linking of composite films was carried out at different temperatures. The formation of amide linkage induced through heating was observed by Fourier Transform Infrared (FT-IR) and x-ray photoelectron spectroscopy (XPS). The cross-linking of nanocomposites (PAH/PAA/PAH/saponite)<sub>10</sub> showed 60% decrease in permeability of oxygen when compared with the pristine PET substrate film. In contrast, water permeability

\*Correspondence: Jayant Kumar, Center for Advanced Materials, Polymer Science Program, Departments of Chemistry and Physics, University of Massachusetts, Lowell, MA 01854, USA;

1401

DOI: 10.1081/MA-200035343  
Copyright © 2004 by Marcel Dekker, Inc.

1060-1325 (Print); 1520-5738 (Online)  
www.dekker.com

Request Permissions / Order Reprints  
powered by **RIGHTS**

of the nanocomposite membrane was not affected by heating temperature and deposition cycles.

*Key Words:* Polymer-layered silicate nanocomposites (PLSNs); Gas barrier properties; Permeability; Cross-linking; Electrostatic layer-by-layer (ELBL) assembly.

## INTRODUCTION

During the last decade, the development of a novel type of composite material led to a significant improvement of mechanical, thermal, and vapor transport properties of films and coatings. Polymer-layered silicate nanocomposites (PLSNs)<sup>1-31</sup> have recently attracted much attention in many applications<sup>4-71</sup> extending to the automotive, electrical, biomedical, and packaging industries.

Of particular interest in PLSNs are nanocomposites in which one or more components have been oriented with respect to the direction of flow.<sup>18,91</sup> Among fabrication methods for PLSNs, electrostatic layer-by-layer (ELBL) assembly<sup>10,111</sup> is a relatively simple, powerful, and versatile method for the preparation of novel surfaces and functional thin films with ordered nanostructures. Such nanoassemblies favor development of novel materials for films with potential applications in several areas such as biosensor,<sup>121</sup> enzyme immobilization,<sup>131</sup> permselectivity,<sup>141</sup> diffusion barrier membranes,<sup>161</sup> and surface patterning.<sup>151</sup>

The permeability<sup>181</sup> ( $P$ ) of polymers with respect to a given permeant depends on both the translational diffusion ( $D$ ) and solubility ( $S$ ) constants.

$$P = D \times S \quad (1)$$

As is well known,  $D$  increases with temperature and with the strength of attractive interactions between the polymer and the permeant. Permeability decreases with the increase in the size of the permeant and with the decrease in the free volume of the polymer. Consequently, the increase in the degree of crystallinity of a polymer, the increase in its chain order, the increase in the degree of cross-linking, and packing density, as well as a compact morphology, are all structural factors enhancing the barrier properties of a polymer. Polymers which interact strongly with permeants favor permeability and conversely polymers interacting poorly with a given permeant will decrease permeation and therefore enhance the barrier properties of the composite *vis-a-vis* a given permeant.

It is, therefore, obvious that cross-linking of polyelectrolyte films contributes to the increase in vapor and gas barrier properties of nanocomposite films while simultaneously improving their pH stability, heat resistance, and mechanical properties.<sup>1161</sup>

A variety of high performance organic-inorganic hybrid materials can be produced due to synergistic effects of individual organic and inorganic components. They can be used directly in industry for coating various substrates such as cellulose acetate (CA), poly(ethylene terephthalate) (PET), Nafion<sup>TM</sup>, etc., as well as free-standing<sup>1171</sup> nanocomposite thin films.

In this study, enhancement of barrier properties of PET films by ELBL assembly is described. The effect of cross-linking of composite films on barrier properties *vis-a-vis* oxygen and water vapor permeation is also reported.

## EXPERIMENTAL

## Materials

Saponite was provided by Source Clay Minerals Respository, University of Missouri. Poly(allylamine hydrochloride) (PAH) ( $M_w = 70,000$ ) and Poly(acrylic acid) (PAA) ( $M_w = 50,000$ ) (Fig. 1) were used as received from Aldrich and Polysciences, Inc., respectively. The pH values of the deposition solutions, PAH and PAA, were adjusted to 2.5 and 4.5 using dilute HCl and NaOH solutions, respectively. Samples for  $O_2$  permeability measurements were made on PET films obtained from DuPont Chemicals (Mylar<sup>®</sup> LB). The thickness of the films was 12  $\mu\text{m}$ .

## Preparation of Saponite Nanoplatelets

Saponite particles were dispersed in deionized water at a concentration of 0.2 wt%. The dispersion was shaken for 1 day and then sonicated for 4–6 hr. After the larger unexfoliated particles (or aggregates) were separated by centrifugation, the resulting clear supernatant was used for the multilayer build up.<sup>1181</sup>

## Multilayer Nanocomposite Film Formation on PET Films via Layer-by-Layer Deposition

Saponite/polyelectrolyte multilayers were deposited on PET sheets without any pre-treatment of the PET surface. Overall, the process of the self-assembly consisted of the cyclic repetition of four steps: (1) immersion of the substrate into an aqueous 10 mM solution of PAH or PAA for 5 min, (2) rinsing with deionized water in three different containers for 1 min between different polymer solutions and drying under a stream of dry nitrogen, (3) immersion into an aqueous dispersion of saponite for 1 min, and (4) final rinsing with deionized water for 1 min and drying under a stream of dry nitrogen. The buildup sequence and deposition cycles,  $n$ , of the film are referred to as (PAH/PAA/PAH/Saponite) $_n$ . For cross-linking, the membranes were placed in heating oven which was purged with  $N_2$  and heated to the desired temperature. The heating continued

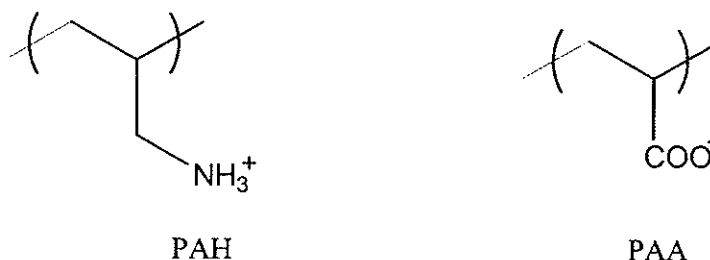


**Figure 1.** The structure of polyelectrolytes used for preparation of multilayer polymer-clay nanocomposites.

at the desired temperature (130–190°C) for 2 hr under N<sub>2</sub> purging. Ultrathin free-standing nanocomposite films were also obtained by layer-by-layer (LBL) assembly as described in the literature.<sup>116,191</sup> PAH, PAA, and exfoliated saponite particles were alternately deposited on a glass plate coated with CA, and the CA substrate was then dissolved in acetone in order to peel the nanocomposite films off the glass. To obtain Fourier Transform Infrared (FT-IR) spectrum of crossed-linked films, the free-standing film was heated to the desired temperature for 2 hr.

### Characterization and Measurement

The thickness of the assembled films was measured using an ellipsometer (AutoEL-III, Rudolph Research, USA) equipped with a 632.8 nm He–Ne laser at an incident angle of 70° and a Dektak profilometer. The IR spectra were recorded on a Perkin–Elmer 1760X FT-IR spectrometer. XPS measurements were performed in a VG ESCALAB MK II photoelectron spectrometer equipped with an Mg K $\alpha$  X-ray source.

Oxygen transmission rate measurements were performed according to ASTM D-3985. An Oxtran Modular System by MOCON, was used to test the samples. The sensor used to detect O<sub>2</sub> was a Coulox sensor. Samples were run at 0% relative humidity, at 23°C. The sample size was 5 × 5 cm<sup>2</sup>. The test gas (O<sub>2</sub>) flow rate was 20 standard cubic centimeters per minute (sccm) and the carrier gas (N<sub>2</sub>/H<sub>2</sub> mix) flow rate was 10 sccm. The O<sub>2</sub> concentration was 100%. Water vapor transmission rate measurements were performed according to ASTM F-1249. A Permatran-W Modular System by MOCON, was used to test the samples. The sensor used to detect O<sub>2</sub> was a modulated infrared sensor. Samples were run at 37.8 °C (90% relative humidity). The sample size was 5 cm<sup>2</sup>. The test gas (humidified N<sub>2</sub>) flow rate was 100 sccm and the carrier gas (dry N<sub>2</sub>) flow rate was 100 sccm.

## RESULTS AND DISCUSSION

### ELBL Assembly of PAH, PAA, and Saponite

The polyelectrolytes, PAH and PAA and exfoliated saponite nanoparticles were deposited on the untreated PET substrate film by sequential LBL deposition. It was proposed that the major adhesion force between polyelectrolytes and clay is hydrophobic interaction.<sup>1201</sup> It was found by ellipsometry and Dektak that the thickness of polymer and clay layers increased with the number of deposition cycles. It was reported that the thickness of LBL assembled films of PAH and PAA depends on the pH of deposition solution.<sup>1211</sup> The pH of solutions was adjusted to 2.5 and 4.5, respectively. This minimized the thickness of produced composite film with molecular order.

### Characterization of Cross-linking by FT-IR and XPS

To induce thermally cross-linked films, the composite membranes were heated to different temperatures (130 °C, 160 °C, and 190 °C). FT-IR shows that before

heating, the dominant peaks are due to COOH carbonyl, asymmetric, and symmetric stretches ( $1725$ ,  $1550$ , and  $1450\text{ cm}^{-1}$ , respectively, in Fig. 2).<sup>1161</sup> After heating, the carbonyl peak at  $1725\text{ cm}^{-1}$  disappeared and a new amide peak at  $1650\text{ cm}^{-1}$  appeared. Heating at  $190^\circ\text{C}$  for 2 hr was enough for cross-linking of the free-standing nanocomposite films. Furthermore, XPS showed that after heating at (Fig. 3)  $190^\circ\text{C}$  for 2 hr, binding energy of  $\text{N}_{1s}$  was shifted to  $401\text{ eV}$  (amino nitrogen) from  $403\text{ eV}$  (ammonium nitrogen).<sup>1221</sup>

### Oxygen and Water Permeability Properties

Permeability of nanocomposites (coated on PET film) to oxygen was measured after heating the composite film at different temperatures (Fig. 4). Pristine PET film was annealed at similar temperatures to see the crystallinity effect on permeability.<sup>181</sup> Figure 4 shows that heating above  $130^\circ\text{C}$  for 2 hr induced only 20% decrease in permeability in case of uncoated PET film. The nanocomposites (PAH/PAA/PAH/saponite)<sub>10</sub> deposited on PET film showed almost 60% decrease in oxygen permeability when compared with uncoated PET film. The permeability to oxygen was almost leveled off after annealing at  $130^\circ\text{C}$  for 2 hr. It is believed that at a high temperature PET film shows some defects on the substrate because it became brittle and, in some cases, had wrinkles at high temperature. The effect of number of deposition cycles on permeability was also investigated at  $190^\circ\text{C}$  for 2 hr heating. It was found that the permeability decrease leveled off at 10 cycles of composite film deposited on the PET substrate (Fig. 5).

Unlike oxygen barrier properties of the nanocomposite membranes, the permeation rate of water vapor was not much affected by heating temperature (Fig. 6) and film thickness (Fig. 7). Also, cross-linking of PAH and PAA sandwiched between lamellae of aluminosilicate does not affect the water permeability very much. This is believed to be

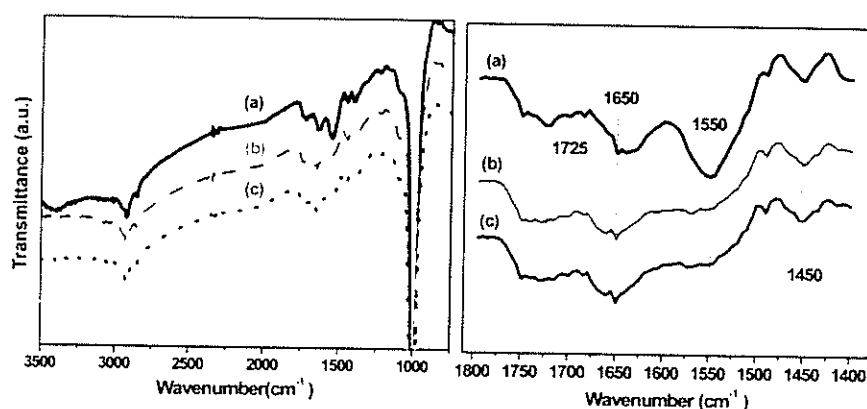


**Figure 2.** The FT-IR spectra of the nanocomposites, (PAH/PAA/PAH/clay)<sub>20</sub> before heating (a) and at  $190^\circ\text{C}$  for 1 hr (b); 2 hr; (c); 3 hr (d).

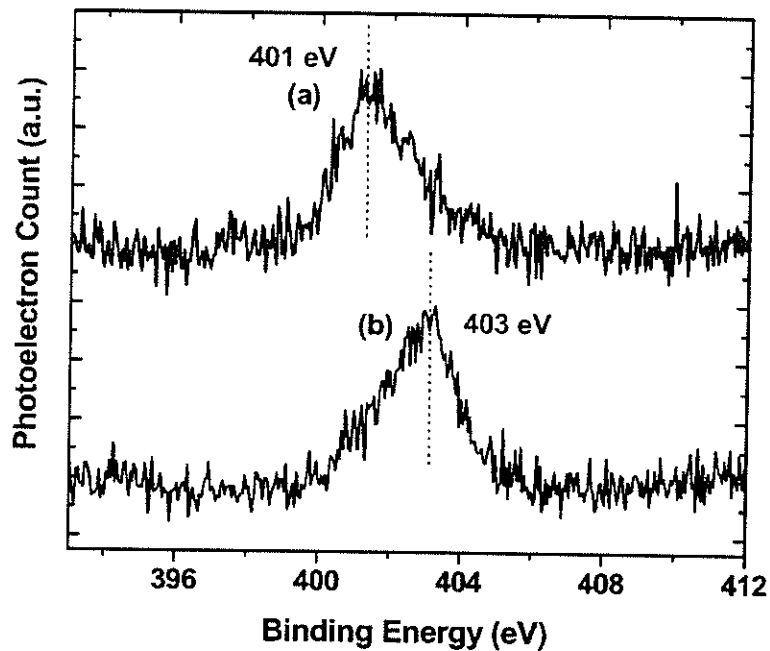


Figure 3. XPS spectra of cross-linked nanocomposite, (PAH/PAA/PAH/clay)<sub>10</sub>. Film after heating at 190°C for (a) 2 hr and (b) before heating.

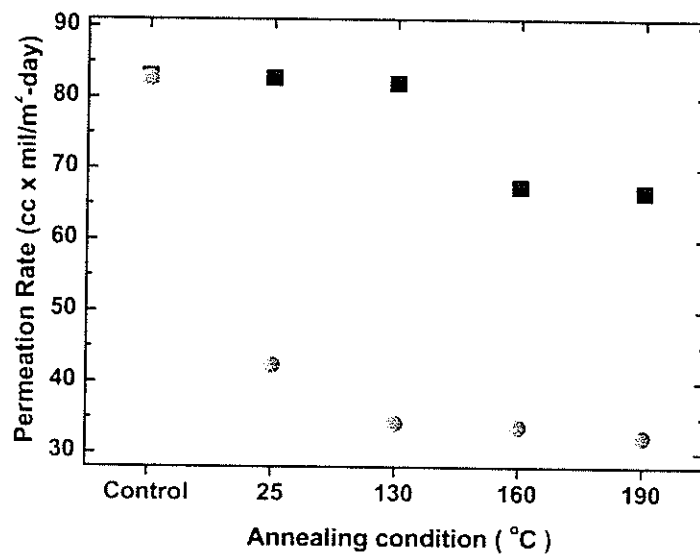


Figure 4. The dependence of oxygen permeation rate of PET film (■) (untreated, but annealed) and the cross-linked nanocomposite, (PAH/PAA/PAH/clay)<sub>10</sub> (●) on the PET substrate (control) at different heating temperatures but same heating time (2 hr).

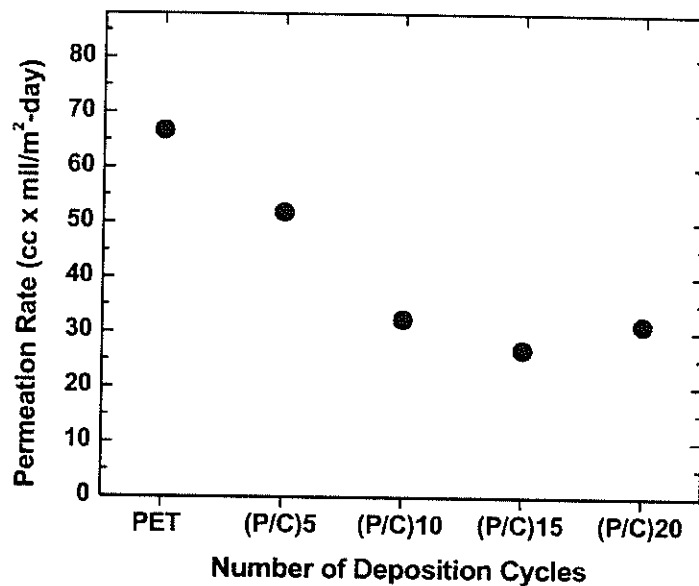


Figure 5. Dependence of the oxygen permeation rate of the cross-linked nanocomposite, (PAH/PAA/PAH/clay)<sub>10</sub> through PET substrate on the number of deposition cycles (all films are annealed at 190°C for 2 hr).

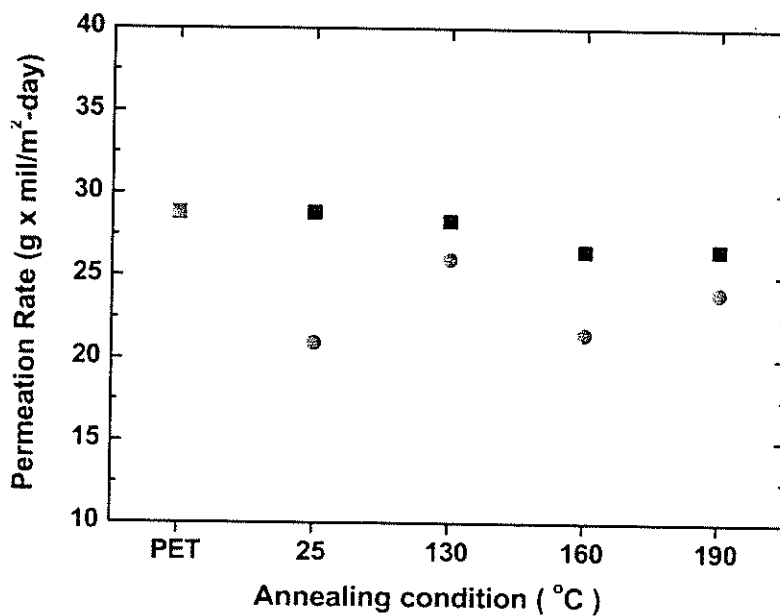
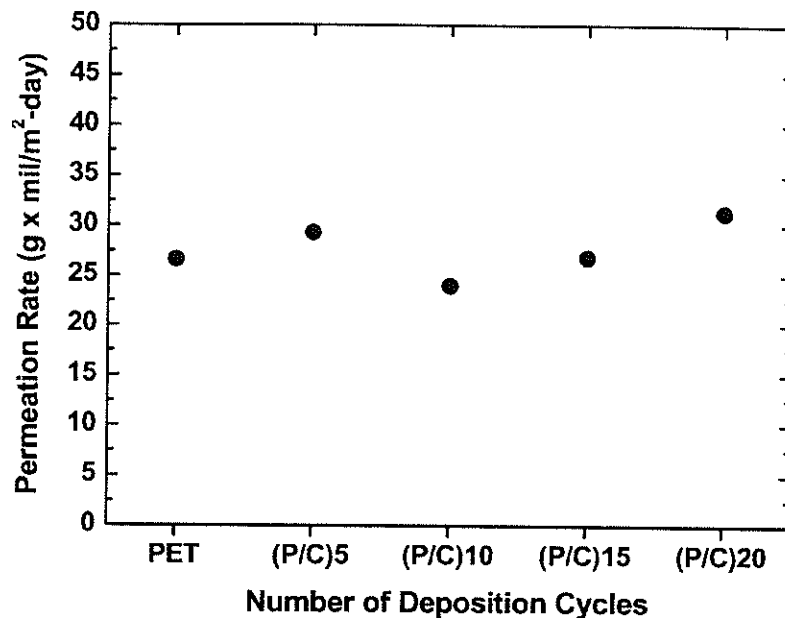


Figure 6. Dependence of the water permeation rate of PET film (untreated, but annealed) (■) and the cross-linked nanocomposite, (PAH/PAA/PAH/clay)<sub>10</sub> through PET substrate (●) on different heating temperatures but same heating time (2 hr).



*Figure 7.* Dependence of the water permeation rate of the cross-linked nanocomposite, (PAH/PAA/PAH/clay)<sub>10</sub> through PET substrate on the number of deposition cycles (all films are annealed at 190°C for 2 hr).

due to hydrophilicity of the clay and of the polyelectrolytes as well as the polarity difference between oxygen and water.<sup>[20]</sup>

## CONCLUSIONS

Organic-inorganic hybrid nanocomposite membranes deposited on a PET substrate were prepared by LBL assembly. The ultrathin cross-linked nanocomposite coating on PET displayed high oxygen barrier properties when compared with the substrate film. Cross-linking of multilayered nanocomposites deposited on a PET substrate film provides enhancement of mechanical integrity and gas barrier property. The procedure outlined earlier can be potentially applied to the membranes such as CA, EVOH, Nafion<sup>®</sup>, and plasma treated membranes.

## ACKNOWLEDGMENTS

Professor J.E. Whitten and Ms. J. Lucciarini are greatly acknowledged for discussion of XPS data and gas barrier property measurements, respectively. We also appreciate the PET film donation from Bobby Reekers in Dupont Co. This work was funded by US Army RDECOM. Finally, this paper is dedicated to the memory of Sukant Tripathy.

## REFERENCES

1. Pinnavaia, T.J.; Beal, G.W., Eds. *Polymer-Clay Nanocomposites*; John Wiley & Sons: New York, 2001.
2. Alexandre, M.; Dubois, P. Polymer-layered silicate nanocomposites: preparation, properties and uses of a new class of materials. *Mater. Sci. Eng. Rep.* **2000**, *R28*, 1.
3. Blumstein, A. Polymerization of adsorbed monolayers. II. Thermal degradation of the inserted polymer. *J. Polym. Sci. Part A* **1965**, *3*, 2665–2672.
4. Giannelis, E.P. Polymer layered silicate nanocomposites. *Adv. Mater.* **1996**, *8*, 29.
5. Kojima, Y.; Usuki, A.; Kawasumi, M.; Okada, A.; Fukushima, Y.; Kurauchi, T.; Kamigaito, O. Mechanical properties of nylon 6-clay hybrid. *J. Mater. Res.* **1993**, *6*, 1185–1189.
6. Ku, B.C.; Blumstein, A.; Samuelson, L.A.; Kumar, J.; Kim, D.W. Barrier properties of ordered multilayer polymer nanocomposites. In *Encyclopedia of Nanoscience and Nanotechnology*; Schwarz, J.A., Contescu, C., Putyera, K., Eds.; Marcel Dekker: NY, 2004; Vol. 1, 213–225.
7. Gilman, J.W. Flammability and thermal stability studies of polymer layered-silicate (clay) nanocomposites. *Appl. Clay Sci.* **1999**, *15*, 31–49.
8. Pauly, S. Permeability and diffusion data. In *Polymer Handbook*, 4th Ed.; Brandrup, J., Immergut, E.H., Grulke, E.A., Eds.; John Wiley & Sons Inc.: NY, 1999; 543–569.
9. Bharadwaj, R.K. Modeling the barrier properties of polymer-layered silicate nanocomposites. *Macromolecules* **2001**, *34*, 9189–9192.
10. Kleinfeld, E.R.; Ferguson, G.S. Stepwise formation of multilayered nanostructural films from macromolecular precursors. *Science* **1994**, *265*, 370–373.
11. Decher, G. Fuzzy nanoassemblies: toward layered polymeric multicomposites. *Science* **1997**, *77*, 1232–1237.
12. Willner, I.; Katz, E. Integration of layered redox proteins and conductive supports for bioelectronic applications. *Angew. Chem. Int. Ed.* **2000**, *39*, 1181–1218.
13. Lvov, Y.M. Polyion-protein nanocomposite films. In *Encyclopedia of Surface and Colloid Science*; Hubbard, A.T., Ed.; Marcel Dekker, Inc.: NY, 2002; Vol. 3, 4162–4171.
14. Tieke, B. Polyelectrolyte multilayer membranes for materials. In *Handbook of Polyelectrolytes and their Applications*; Tripathy, S.K., Kumar, J., Nalwa, H.S., Eds.; American Scientific Publishers: CA, 2002; Vol. 3, 115–124.
15. Hammond, P.T. Recent explorations in electrostatic multilayer thin film assembly. *Curr. Opin. Colloid. Interface Sci.* **2000**, *4*, 430–442.
16. Harris, J.J.; Derose, P.M.; Breuning, M.L. Synthesis of passivating, nylon-like coatings through crosslinking of ultrathin polyelectrolyte films. *J. Am. Chem. Soc.* **1999**, *121*, 1978–1979.
17. Mamedov, A.A.; Kotov, N.A. Free-standing layer-by-layer assembled films of magnetite nanoparticles. *Langmuir* **2000**, *16*, 5530–5533.
18. Kim, D.W.; Blumstein, A.; Tripathy, S.K. Nanocomposite films derived from exfoliated functional aluminosilicate through electrostatic layer-by-layer assembly. *Chem. Mater.* **2001**, *13*, 1916–1922.
19. Kim, D.W.; Blumstein, A.; Kumar, J.; Samuelson, L.A.; Kang, B.; Sung, C. Ordered multilayer nanocomposites prepared by electrostatic layer-by-layer assembly between aluminosilicate nanoplatelets and substituted ionic polyacetylenes. *Chem. Mater.* **2002**, *14*, 3925–3929.

20. Kotov, N.A.; Maganov, S.; Tropsha, E. Layer-by-layer self-assembly of aluminosilicate-polyelectrolyte composites: mechanism of deposition, crack resistance, and perspectives for novel membrane materials. *Chem. Mater.* **1998**, *10*, 886–895.
21. Yoo, D.; Shiratori, S.S.; Rubner, M.F. Controlling bilayer composition and surface wettability of sequentially adsorbed multilayers of weak polyelectrolytes. *Macromolecules* **1998**, *31*, 4309–4318.
22. Wagner, C.D.; Riggs, W.M.; Davis, L.E.; Moulder, J.F.; Muilenberg, G.E. *Handbook of X-Ray Photoelectron Spectroscopy*; Perkin-Elmer: Eden Prairie, MN, 1979.